Proton-Λ correlations in central Pb+Pb collisions at sqrt[s_{NN}]=17.3 GeV

T. Anticic *et al.* (NA49 Collaboration)

Proton – Lambda Correlations in Central Pb+Pb Collisions at $\sqrt{s_{\mathrm{NN}}} = 17.3$ GeV

T. Anticic,[22] B. Baatar,[8] D. Barna,[4] J. Bartke,[6] H. Beck,[9] L. Betev,[10] H. Białkowska,[19]

C. Blume,[9] M. Bogusz,[21] B. Boimska,[19] J. Book,[9] M. Botje,[1] P. Bunčić,[10] T. Cetner,[21]

P. Christakoglou,[1] P. Chung,[18] O. Chvála,[14] J.G. Cramer,[15] V. Eckardt,[13] Z. Fodor,[4]

P. Foka,[7] V. Friese,[7] M. Gaździcki,[9, 11] K. Grebieszkow,[21] C. Höhne,[7] K. Kadija,[22]

A. Karev,[10] V.I. Kolesnikov,[8] M. Kowalski,[6] D. Kresan,[7] A. László,[4] R. Lacey,[18]

M. van Leeuwen,[1] M. Maćkowiak,[21] M. Makariev,[17] A.I. Malakhov,[8] M. Mateev,[16]

G.L. Melkumov,[8] M. Mitrovski,[9] St. Mrówczyński,[11] V. Nicolic,[22] G. Pálla,[4]

A.D. Panagiotou,[2] W. Peryt,[21] J. Pluta,[21] D. Prindle,[15] F. Pühlhofer,[12] R. Renfordt,[9]

C. Roland,[5] G. Roland,[5] M. Rybczyński,[11] A. Rybicki,[6] A. Sandoval,[7] N. Schmitz,[13]

T. Schuster,[9] P. Seyboth,[13] F. Siklér,[4] E. Skrzypczak,[20] M. Słodkowski,[21] G. Stefanek,[11]

R. Stock,[9] H. Ströbele,[9] T. Susa,[22] M. Szuba,[21] M. Utvić,[9] D. Varga,[3] M. Vassiliou,[2]

G.I. Veres,[4] G. Vesztergombi,[4] D. Vranić,[7] Z. Włodarczyk,[11] and A. Wojtaszek-Szwarc[11]

(The NA49 Collaboration)

[1]NIKHEF, Amsterdam, Netherlands.

[2]Department of Physics, University of Athens, Athens, Greece.

[3]Eötvös Loránt University, Budapest, Hungary.

[4]KFKI Research Institute for Particle and Nuclear Physics, Budapest, Hungary.

[5]MIT, Cambridge, USA.

[6]H. Niewodniczański Institute of Nuclear Physics,

Polish Academy of Sciences, Cracow, Poland.

[7]Gesellschaft für Schwerionenforschung (GSI), Darmstadt, Germany.

[8]Joint Institute for Nuclear Research, Dubna, Russia.

[9]Fachbereich Physik der Universität, Frankfurt, Germany.

[10]CERN, Geneva, Switzerland.

[11]Institute of Physics, Jan Kochanowski University, Kielce, Poland.

[12]Fachbereich Physik der Universität, Marburg, Germany.

[13]Max-Planck-Institut für Physik, Munich, Germany.

[14]Inst. of Particle and Nuclear Physics,

Charles Univ., Prague, Czech Republic.

[15]Nuclear Physics Laboratory, University of Washington, Seattle, WA, USA.

[16]Atomic Physics Department, Sofia Univ. St. Kliment Ohridski, Sofia, Bulgaria.

[17]Institute for Nuclear Research and Nuclear Energy, BAS, Sofia, Bulgaria.

[18]Department of Chemistry, Stony Brook Univ. (SUNYSB), Stony Brook, USA.

[19]Institute for Nuclear Studies, Warsaw, Poland.

[20]Institute for Experimental Physics,

University of Warsaw, Warsaw, Poland.

[21]Faculty of Physics, Warsaw University of Technology, Warsaw, Poland.

[22]Rudjer Boskovic Institute, Zagreb, Croatia.

Abstract

The momentum correlation between protons and lambda particles emitted from central Pb+Pb collisions at $\sqrt{s_{\mathrm{NN}}} = 17.3$ GeV was studied by the NA49 experiment at the CERN SPS. A clear enhancement is observed for small relative momenta ($q_{\mathrm{inv}} < 0.2$ GeV). By fitting a theoretical model, which uses the strong interaction between the proton and the Λ in a given pair, to the measured data a value for the effective source size is deduced. Assuming a static Gaussian source distribution we derive an effective radius parameter of $R_{\mathrm{G}} = 3.02 \pm 0.20(\mathrm{stat.})^{+0.44}_{-0.16}(\mathrm{syst.})$ fm.

I.   INTRODUCTION

Heavy-ion collisions at ultra-relativistic energies produce strongly interacting matter under extreme conditions. The main goal is to create in these reactions a state in which the confinement of quarks and gluons inside hadrons is no longer effective, the so-called quark-gluon plasma. This strongly compressed matter undergoes a rapid expansion with a drop of temperature and energy density. Two-particle momentum correlations provide unique information on the size and dynamic evolution of this fireball and are therefore a widely employed observable in heavy-ion physics. Usually correlations of identical charged pions are studied which, due to the high available statistics, allow a multi-dimensional study of radius parameters [1–3]. Less frequently two-proton correlations are analyzed [4–7], although only one-dimensionally. Moreover, the large abundance of strange particles produced in heavy-ion collisions allows to study also two particle correlations between pairs of strange particles or pairs of strange and non-strange particles. For example the correlations of identical kaons were investigated at the CERN-SPS [8] as well as at RHIC [9]. In this paper we report on the measurement of the $p - \Lambda$ correlation function in central Pb+Pb collisions at $\sqrt{s_{\mathrm{NN}}} = $ 17.3 GeV at the CERN-SPS.

It was suggested that also the momentum correlation between Λ and protons can be employed to measure the size of the emitting source [10]. The correlation function of $p - \Lambda$ pairs is only affected by the strong interaction between the particles. This distinguishes $p - \Lambda$ correlations from the two-proton case, for which the correlation function is dominated by the repulsive Coulomb interaction and the Fermi-Dirac statistics at low relative momenta. Both effects are absent in the $p - \Lambda$ correlation function, which should therefore be more sensitive to large source sizes [10]. However, the knowledge of the strong interaction between protons and Λ is necessary to relate the strength of the correlation to the size of the emitting source. There is a substantial set of data available on low-energy elastic Λ p scattering [11–13], and on $K^- d \to \Lambda \, p \, \pi^-$ [14–16], as well as $pp \to p K^+ \Lambda$ [17, 18] reactions. Also Λ hypernuclei provide important information on the Λ nucleon interaction. Based on this data many theoretical analyses derived $p - \Lambda$ scattering lengths and effective interaction ranges [19–25] which can be used to calculate the $p - \Lambda$ correlation function.

A preliminary study by the NA49 experiment at the SPS was reported in [26]. Here we describe the final results of a new and improved analysis [27]. Similar studies of $p - \Lambda$

correlations in heavy ion collisions were performed at lower [7, 28] and higher [29] center-of-mass energies, allowing to investigate the evolution of $p - \Lambda$ correlations with $\sqrt{s_{NN}}$.

II. DATA ANALYSIS

The data presented here were measured by the NA49 experiment at the CERN SPS. A detailed description of the experimental setup can be found in [30]. Charged particles produced by interactions of the Pb beam in a thin Pb-foil target are tracked with four large-volume Time Projection Chambers (TPCs). Two TPCs are placed inside two superconducting dipole magnets, while the other two are situated outside of the magnetic field. Since the latter measure long pieces of the particle tracks, they allow a precise determination of the specific energy loss dE/dx inside the detector gas (typical resolution of 4 %) and thus particle identification in a large region of phase-space. Additional particle identification is provided around mid-rapidity by Time-Of-Flight detectors. A Zero Degree Calorimeter is used to measure the energy in the projectile fragmentation region from which the centrality of the reaction can be deduced. This analysis is based on $2.8 \cdot 10^6$ Pb+Pb events at $\sqrt{s_{NN}} = 17.3$ GeV recorded in the year 2000, which cover the 23.5 % most central part of the total inelastic cross section, corresponding to an averaged number of wounded nucleons of $\langle N_w \rangle = 262$.

A. Λ reconstruction

The Λ hyperons are detected via their charged decay $\Lambda \rightarrow p\pi^-$, using the same methods as described in [31, 32]. The Λ reconstruction is done by forming pairs of positively and negatively charged tracks and extrapolating them towards the main interaction vertex. The positively (negatively) charged tracks are required to have at least 50 (30) reconstructed points. Pairs with a distance of closest approach of less than 0.5 cm anywhere between the position of the first measured point on the tracks and the target plane are considered as V^0 candidates. Assigning proton and pion masses to the positively and negatively charged decay particle, the invariant mass of a Λ candidate is calculated. A significant reduction of the combinatorial background can be achieved by applying several selection criteria to the Λ candidates. In this analysis it is required that the secondary vertex is separated by at least
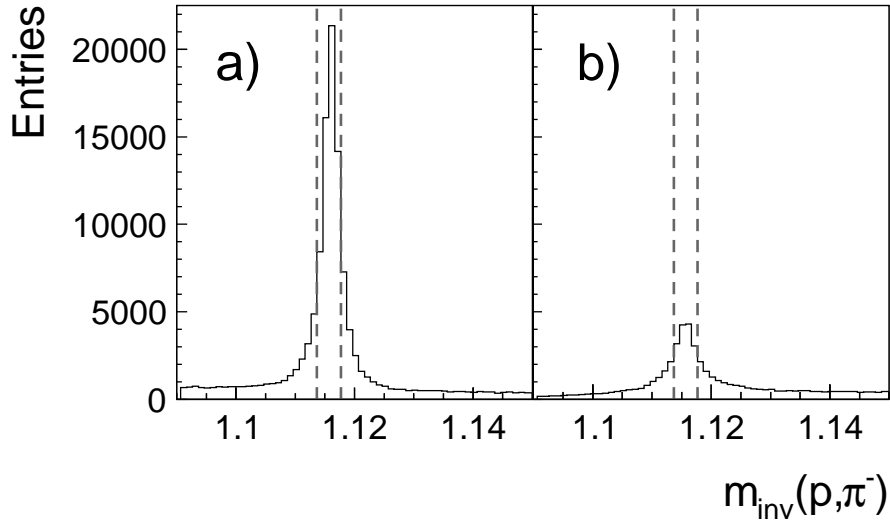
4

FIG. 1: The invariant mass distribution of Λ candidates in two exemplary phase-space bins ((a) $-1.2 < y < -0.4$ and $0.6 < p_{\mathrm{t}} < 1.2$ GeV/c, (b) $-0.4 < y < 0.4$ and $1.8 < p_{\mathrm{t}} < 2.4$ GeV/c) for central Pb+Pb reactions at $\sqrt{s_{\mathrm{NN}}} = 17.3$ GeV. The two vertical lines indicate the mass windows used to define Λ candidates.

25 cm in beam-(z)-direction from the target plane. Additionally, the back-extrapolation of the flight path of the Λ candidate must not deviate from the interaction vertex position in the transverse directions x and y by more than $|\Delta x| = 0.75$ cm and $|\Delta y| = 0.375$ cm. The signal-to-background ratio is further improved by enriching the protons in the sample of positively charged tracks by applying a momentum-dependent cut on the measured energy loss ($\mathrm{d}E/\mathrm{d}x$). An additional $\mathrm{d}E/\mathrm{d}x$ cut on the negatively-charged tracks also allows to reject electrons from photon conversions.

An important point with respect to correlation studies is the requirement that each Λ candidate must be unique. If it happens that a daughter track of a given Λ candidate is also assigned to another one, a strong artificial correlation between both candidates is created which in turn affects the measured $\mathrm{p} - \Lambda$ correlation function. In this analysis it is therefore ensured that any given track is used only once as a daughter track. Similarly, Λ daughters that were not reconstructed as a single track, but as two track pieces (split tracks), will cause a distortion of the measured correlation function. To exclude these tracks it is required that the number of measured points of each accepted track is higher than 50 % of the number of
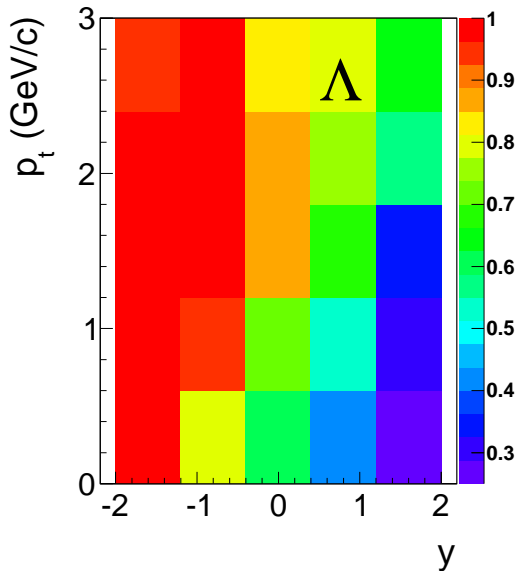
FIG. 2: The purity $P_\Lambda(y, p_\mathrm{t})$ of the selected Λ candidates as function of rapidity y and transverse momentum p_t.

points that this track could maximally have according to its trajectory in the TPCs.

Figure 1 shows the distribution of invariant mass m_{inv} of Λ candidates obtained after assigning the proton (π^-) mass to the positive (negative) daughter track for two intervals of the center-of-mass rapidity y and transverse momentum p_t. Λ are accepted in a mass window $[m_0 - \Delta m, m_0 + \Delta m]$ of a half-width of $\Delta m = 2$ MeV/c^2, where $m_0 = 1.115683$ GeV/c^2 is the literature value for the Λ mass [33]. This mass window was chosen in order to optimize the signal-to-background ratio and reduce the corrections for the signal purity.

The ratio between signal and background inside this mass window and with it the purity of the Λ sample vary over phase-space. A χ^2-fit to the invariant mass distributions in different y and p_t bins was performed in order to determine the relative contributions. The fit function used is the sum of a polynomial for the combinatorial background and a function for the Λ signal. The measured shape of the Λ signal results from a convolution of the resolutions for the single track momenta and the secondary vertex positions and is found to be well described by an asymmetric Lorentz-curve. By subtracting the background function from the measured invariant mass distribution the number of real Λ is determined. Defining the purity P_Λ by the ratio of the number of real Λ to the number of accepted Λ candidates in the chosen mass window one obtains the result shown in Fig. 2. The phase-space averaged
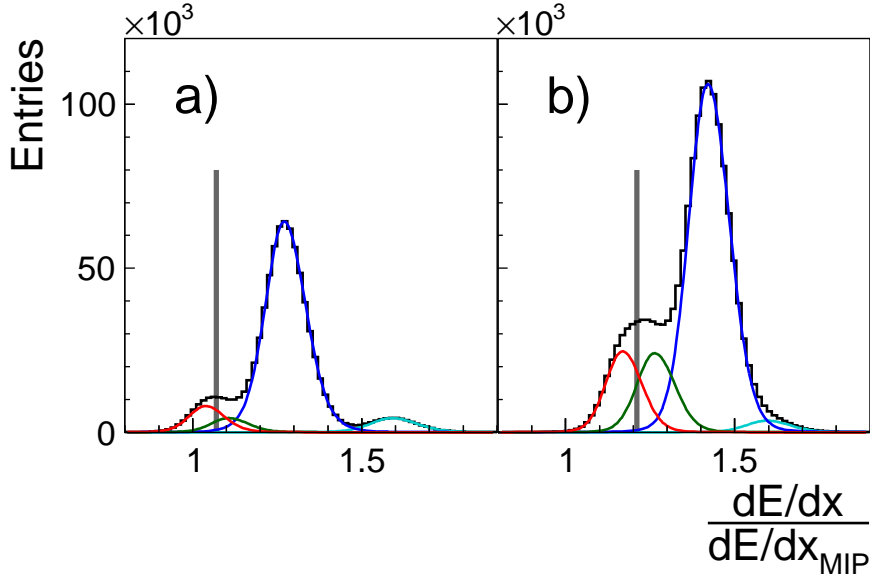
FIG. 3: The dE/dx spectra in two exemplary total momentum bins ((a) $4.0 < p < 5.0$ GeV/c, (b) $12.6 < p < 15.9$ GeV/c) together with their decomposition into contributions from protons, kaons, pions, and electrons (from left to right). Shown is the measured energy loss normalized to the minimum ionizing value dE/dx_{MIP}. The vertical lines represent the upper dE/dx cuts that result in a purity of $P_{\mathrm{p}} = 0.8$.

value of the Λ purity is $\langle P_\Lambda \rangle = 69$ %.

B. Proton reconstruction

Protons are identified via their energy loss dE/dx as measured in the two Main-TPCs. A valid proton track is required to have at least 50 reconstructed points. An additional cut on the impact parameters in the target plane ($|b_{\mathrm{x}}| < 5.0$ cm, $|b_{\mathrm{y}}| < 2.0$ cm) reduces the contribution from secondary tracks. In order to assign the probability of being a proton to a given track, the energy loss spectra measured in bins of total momentum p are fitted by a sum $E(x, p)$ of asymmetric Gaussians using a χ^2 minimizing procedure [34]:

$$E(x,p) = \sum_{i=\mathrm{d,p,K,\pi,e}} A_i(p) \frac{1}{\sum_l n_l} \sum_l \frac{n_l}{\sqrt{2\pi}\,\sigma_{i,l}(p)} \exp\left[-\frac{1}{2}\left(\frac{x - \hat{x}_i(p)}{(1 \pm \delta)\,\sigma_{i,l}(p)}\right)^2\right]. \quad (1)$$

Here, $A_i(p)$ denotes the yield for particle type i, n_l the number of tracks in a given track length interval l, $\hat{x}_i(p)$ the most probable dE/dx values for particle type i, x the measured

$\mathrm{d}E/\mathrm{d}x$ value of the track under consideration, $\sigma_{i,l}(p)$ the width of the Gaussian, and δ the asymmetry parameter. The parameters $A_i(p)$, $\hat{x}_i(p)$, and $\sigma_\pi(p)$ are determined by the fitting procedure in each p bin separately. The widths for the other particles types and different track length bins are derived from the parameter $\sigma_\pi(p)$ for pions: $\sigma_{i,l}(p) = \sigma_\pi(p) \cdot (\hat{x}_i/\hat{x}_\pi)^\alpha (1/\sqrt{l})$. The exponent was determined to be $\alpha = 0.625$ and the parameter δ is fixed to 0.065. Results of the fit procedure for two different total momentum bins are shown in Fig. 3. Since for low particle momenta the energy loss curves of different particle species cross each other and particle identification is thus not possible, a lower cut on the total momentum of $p > 4$ GeV/c is applied. To exclude the region of the Fermi plateau also momenta above 50 GeV/c are discarded. Based on these fits a momentum dependent cut on the measured $\mathrm{d}E/\mathrm{d}x$ values for single tracks is defined such that the accepted tracks always have the same probability of being a proton. For the standard analysis this probability is set to 80 %, equivalent to a constant proton purity $P_\mathrm{p} = 0.8$. As in the case of the Λ decay daughters it is ensured that split tracks are removed from the track sample by rejecting tracks that have less than 55 % of the number of geometrically possible points.

C. Determination of the p $-$ Λ correlation function

The selected Λ and proton candidates are then combined to form p $-$ Λ pairs. In order to avoid trivial auto-correlations a track that is used to reconstruct the Λ candidate is removed from the primary proton sample. The pair distribution $S(q_\mathrm{inv})$ is measured as a function of the generalized invariant relative momentum of the p $-$ Λ pair q_inv, which is defined as the modulus of $\tilde{q} = q - P(qP)/P^2$, with $q = p_\mathrm{p} - p_\Lambda$, $P = p_\mathrm{p} + p_\Lambda$, and $qP = m_\mathrm{p}^2 - m_\Lambda^2$. Here, p_p and p_Λ are the 4-momenta of the proton and the Λ. In the two particle center-of-mass system $\tilde{q}$ reduces to $\{0, 2\vec{k}^*\}$, with $2\vec{k}^*$ being the 3-momentum difference in this reference frame [35].

An event-mixing method that combines proton and Λ candidates taken from different events, is employed for the construction of the uncorrelated background $B(q_\mathrm{inv})$. The measured correlation function is thus defined as:

$$C_\mathrm{meas}(q_\mathrm{inv}) = N\, \frac{S(q_\mathrm{inv})}{B(q_\mathrm{inv})}. \tag{2}$$

The normalization constant N is determined by requiring $C_\mathrm{meas}(q_\mathrm{inv}) = 1$ in the region
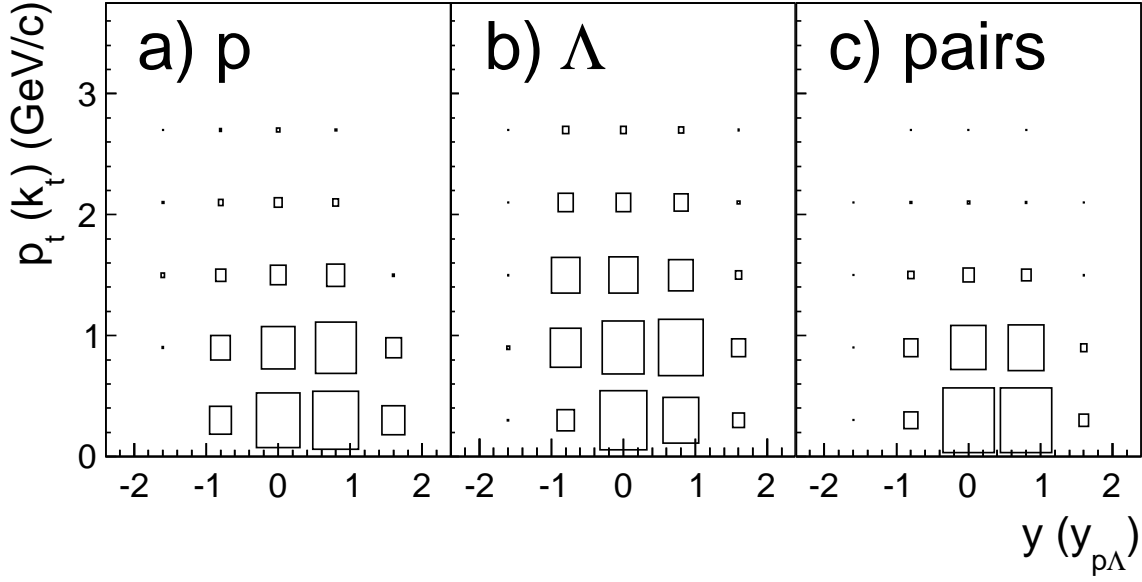
FIG. 4: The phase-space population of protons (a), Λ (b) as a function of rapidity y and transverse momentum p_{t}. The distribution for the resulting $\mathrm{p} - \Lambda$ pairs (c) is shown versus pair rapidity $y_{\mathrm{p}\Lambda} = \frac{1}{2} \ln \frac{E_{\mathrm{p}} + E_{\Lambda} + p_{z,\mathrm{p}} + p_{z,\Lambda}}{E_{\mathrm{p}} + E_{\Lambda} - p_{z,\mathrm{p}} - p_{z,\Lambda}}$ and $k_{\mathrm{t}} = \frac{1}{2} |\vec{p}_{\mathrm{t},\mathrm{p}} + \vec{p}_{\mathrm{t},\Lambda}|$.

$0.2 < q_{\mathrm{inv}} < 0.3$ GeV. Since the reconstruction of real pairs is affected by the limited two-track resolution of the detector [30], a distance cut between the track of the primary proton and the track of the positive Λ decay particle is applied for real pairs as well as for the mixed event pairs. For each pair it is required that the tracks have an average separation of at least 3.0 cm. This average is determined as the arithmetic mean of the track distances determined in planes perpendicular to the beam axis. For each TPC two planes are taken into account. Their distances to the target plane are 160.5 cm, 240.5 cm, 540.0 cm, 620.0 cm, 910.0 cm, and 990.0 cm. Pairs that do not pass the distance cut are discarded.

Figure 4 shows the phase-space population of the accepted protons, Λ, and $\mathrm{p} - \Lambda$ pairs. Averaging over all measured $\mathrm{p} - \Lambda$ pairs we find $\langle k_{\mathrm{t}} \rangle = 0.53$ GeV$/c$ with $k_{\mathrm{t}} = \frac{1}{2} |\vec{p}_{\mathrm{t},\mathrm{p}} + \vec{p}_{\mathrm{t},\Lambda}|$ ($\langle m_{\mathrm{t}} \rangle = 1.18$ GeV with $m_{\mathrm{t}} = \sqrt{k_{\mathrm{t}}^2 + (\frac{1}{2}(m_{\Lambda} + m_{\mathrm{p}}))^2}$).

The measured correlation function can be affected by the finite momentum resolution of the detector. In [3] an extensive investigation of its influence on the radius parameters extracted from correlations of identical charged pions as measured with the NA49 experiment is discussed. Due to the excellent momentum resolution of the NA49 detector, it turned out that the impact is negligible and a correction for this effect is not necessary. Even though
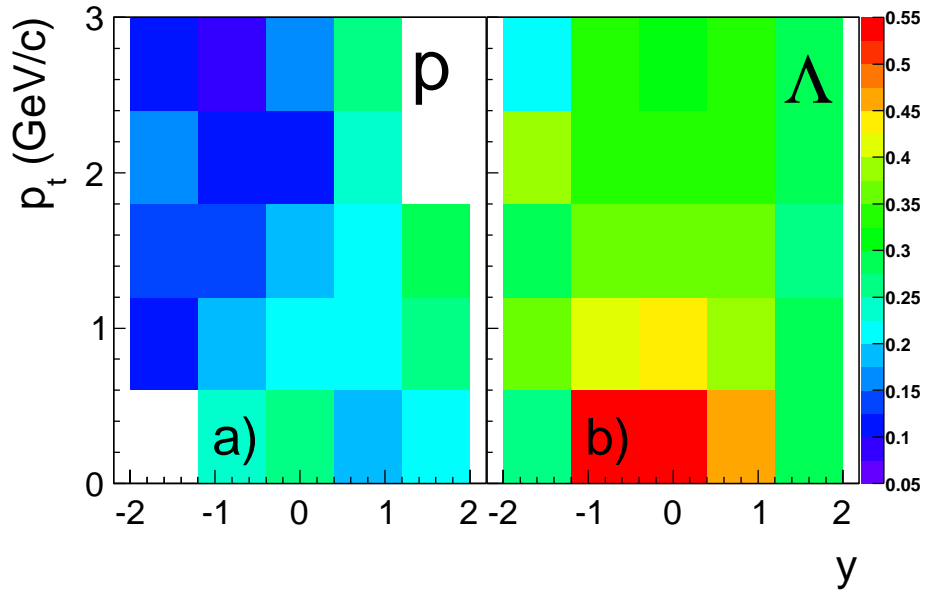
9

FIG. 5: The fraction of protons ($F_{\mathrm{p}}(y, p_{\mathrm{t}})$) (a) and of Λ ($F_{\Lambda}(y, p_{\mathrm{t}})$) (b) originating from feed-down as a function of y and p_{t}.

the momentum resolution for a Λ ($\langle \sigma_{p_{\Lambda}} \rangle \leq 1\%$) is worse than for the primary track, the resulting effect on the measured p $-\Lambda$ correlation function is still clearly smaller than all other systematics effects. Therefore no correction is applied in this analysis.

A substantial fraction of the measured protons and Λ originate from weak and electromagnetic decays of heavier particles (feed-down). In the following it will be assumed that these decay particles are not correlated, because the decays happen long after the thermal freeze-out, and will thus reduce the observed p $-\Lambda$ correlation function. For the Λ the feed-down originates from Ξ^{-}, Ξ^{0}, and Σ^{0} decays, while in case of the protons the decays of Λ, and Σ^{+} contribute. We calculate the fraction of protons and Λ originating from feed-down ($F_{\mathrm{p}}(y, p_{\mathrm{t}})$ and $F_{\Lambda}(y, p_{\mathrm{t}})$) via a simulation procedure. Λ, Ξ^{-}, and Ξ^{0} are generated according to their measured phase-space distributions [31]. The measured Λ include the Σ^{0} which cannot be separated experimentally. For the Ξ^{0} the same input distributions are assumed as for the Ξ^{-} scaled by the ratio Ξ^{0}/Ξ^{-} of the total multiplicities taken from statistical model fits [36]. The daughter tracks of the generated particles are followed through the NA49 detector setup using the Geant3.21 package [37]. The response of the TPCs to the traversing particles is simulated with NA49 specific software. In a next step the simulated raw signals are added to measured raw data and processed by the same reconstruction

program as used for the experimental data. By applying the same cuts as in the normal analysis, the feed-down contributions to the measured Λ and protons are determined. The y and p_t dependences of the feed-down fractions $F_p(y, p_t)$ and $F_\Lambda(y, p_t)$ are summarized in Fig. 5. The phase-space averaged values are $\langle F_p \rangle = 22$ % and $\langle F_\Lambda \rangle = 43$ %.

The final $p - \Lambda$ correlation function $C_{corr}(q_{inv})$ results from the measured $C_{meas}(q_{inv})$ by applying a combined correction factor $\langle K(q_{inv}) \rangle$ for purity and feed-down. This factor is determined by averaging the product $P_p(y_p, p_{t,p}) \, P_\Lambda(y_\Lambda, p_{t,\Lambda})(1 - F_p(y_p, p_{t,p})) \, (1 - F_\Lambda(y_\Lambda, p_{t,\Lambda}))$ over all reconstructed $p - \Lambda$ pair combinations falling into a given bin of relative momentum q_{inv}. The corrected correlation function thus follows from:

$$C_{corr}(q_{inv}) = \frac{C_{meas}(q_{inv}) - 1}{\langle K(q_{inv}) \rangle} + 1. \tag{3}$$

III. RESULTS

In total 70920 $p - \Lambda$ pair candidates, corresponding to 17520 real $p - \Lambda$ pairs (i.e. after correcting for purities and feed-down), with $q_{inv} < 0.2$ GeV were measured. Dividing the signal distribution by the event-mixing background and correcting with the purities and feed-down contribution according to Eqs. (2) and (3) yields the final $p - \Lambda$ correlation function as shown in Fig. 6. The correlation function exhibits a significant enhancement for small q_{inv}. Such a correlation would be expected as the effect of the strong interaction between the proton and the Λ.

A. Fit to theoretical calculation

Since the shape of the momentum correlation function was shown by Wang and Pratt to depend on the size of the emitting source [10], it can be used to extract its radius. The necessary prerequisite is a quantitative knowledge of the $p - \Lambda$ interaction. Here we use a functional form of the theoretical correlation function C_{th} that is based on the model of Lednický and Lyuboshitz [35, 38]. It employs an effective range approximation of the S-wave $p - \Lambda$ interaction. The source size is required to be larger than the effective range of the interaction. The strength of the interaction is defined by four parameters: the effective ranges d_0^S (d_0^T) and the scattering lengths f_0^S (f_0^T) for the singlet $S = 0$ (triplet $S = 1$) state. In our fits we use values of $d_0^S = 2.92$ fm, $d_0^T = 3.78$ fm, $f_0^S = $ -2.88 fm, and $f_0^T = $ -1.8 fm,
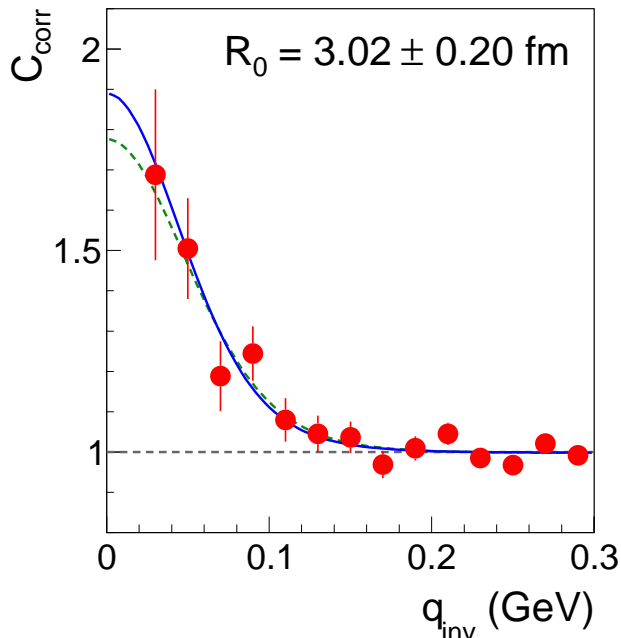
FIG. 6: The corrected p$-\Lambda$ correlation function for central Pb+Pb reactions at $\sqrt{s_{\mathrm{NN}}} = 17.3$ GeV, shown as a function of the invariant relative momentum q_{inv}. The data represent an average over the whole acceptance of the NA49 experiment. The lines display results of the fit with a theoretical correlation function [35, 38] (see text for details). Only statistical errors are shown.

as suggested in [10]. Under the assumption of unpolarized particle production, the relative contribution of pairs in the singlet and the triplet state is 1 : 3. Furthermore, we use the same spherically symmetric Gaussian spatial distribution $S(\vec{r})$, for both the proton and the Λ source:

$$S(\vec{r}) = \exp\left(-\frac{x^2 + y^2 + z^2}{2R_{\mathrm{G}}^2}\right). \tag{4}$$

Then, the theoretical correlation function C_{th} assumes the functional form as quoted in reference [29]. By fitting it to the data one obtains the effective radius parameter R_{G} and an additional parameter λ that takes possible reductions of the height of the correlation into account:

$$C_{\mathrm{fit}}(q_{\mathrm{inv}}) = \lambda\left(C_{\mathrm{th}}(q_{\mathrm{inv}}) - 1\right) + 1. \tag{5}$$

These reductions occur, if the correction for the particle purities and the feed-down, as defined in Eq. (3), are insufficient. If both parameters are left to vary freely, the best fit is obtained for $R_{\mathrm{G}} = 2.70 \pm 0.60(\mathrm{stat.})$ fm and $\lambda = 0.77 \pm 0.38(\mathrm{stat.})$ (green dashed line
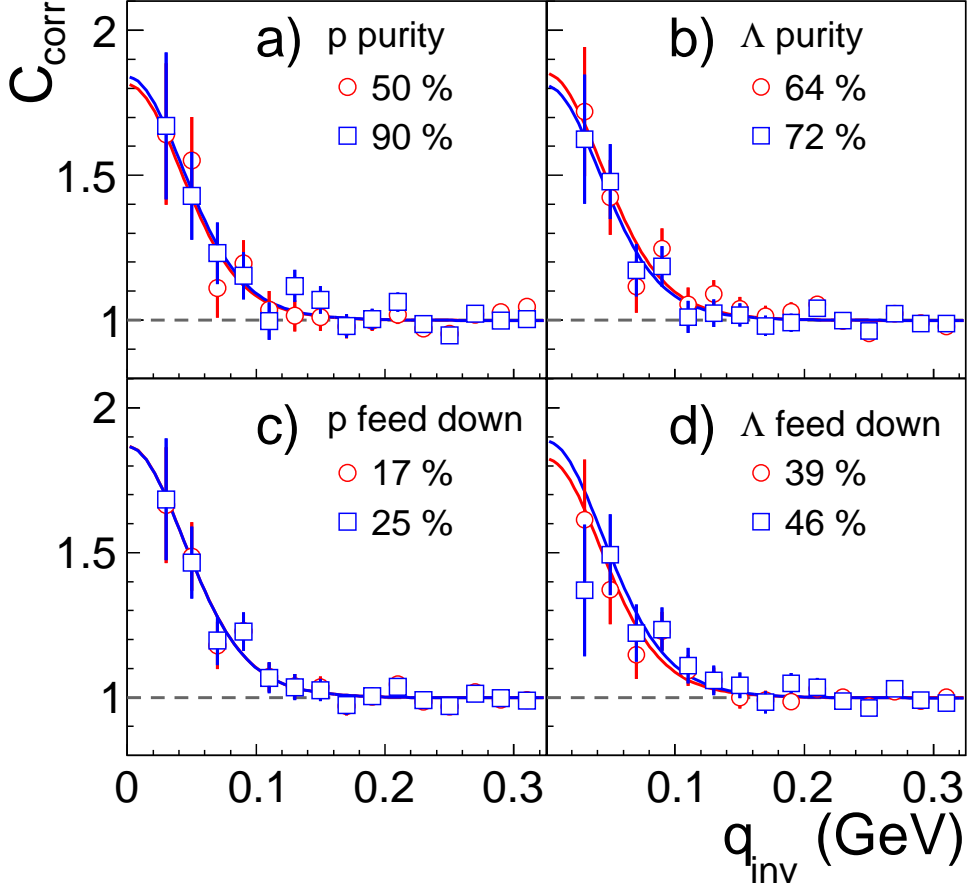
FIG. 7: The corrected p$-\Lambda$ correlation function $C_{\rm corr}(q_{\rm inv})$ for central Pb+Pb reactions at $\sqrt{s_{\rm NN}} = 17.3$ GeV shown as a function of the invariant relative momentum $q_{\rm inv}$ for different purities of protons (a) and Λ (b), as well as different feed-down contributions to protons (c) and Λ (d) (see text). The lines display the results of fits with a theoretical correlation function [35, 38].

in Fig. 6). The agreement within errors of the fitted λ value with unity underlines the consistency of the correction procedure. This justifies to fix $\lambda = 1$ and to use only $R_{\rm G}$ as a free parameter, which reduces the resulting error. With this constraint we obtain $R_{\rm G} = 3.02 \pm 0.20 {\rm (stat.)}$ fm (blue solid line in Fig. 6).

B. Systematic uncertainties

Systematic errors arise both in the extraction of the correlation function and in the theoretical model. The former uncertainties were studied by making small changes in the analysis procedure. By varying the corresponding cuts on the measured energy loss used to

13

identify the primary protons, as well as the decay protons of the Λ candidates, the particle purities $P_{\mathrm{p}}(p_{\mathrm{p}})$ and $P_{\Lambda}(y_{\Lambda}, p_{\mathrm{t},\Lambda})$ can be varied to a certain extent. This changes the measured correlation function $C_{\mathrm{meas}}(q_{\mathrm{inv}})$. However, after applying the appropriate correction factor $\langle K(q_{\mathrm{inv}})\rangle$ the same corrected correlation function should be obtained. Figure 7 shows comparisons of $C_{\mathrm{corr}}(q_{\mathrm{inv}})$ for different proton (Fig. 7,a)) and Λ purities (Fig. 7,b)). Even though the correction factor changes quite dramatically (≈ 45 % in case of the proton purity), the resulting correlation functions agree quite well. The systematic error on the effective radius parameter R_{G} is derived by taking the maximal difference of R_{G} as obtained by fits to the different correlation functions. It is found that it changes between $2.91 - 3.28$ fm ($2.98 - 3.29$ fm), if the proton (Λ) purity is varied between $50 - 90$ % ($64 - 72$ %).

A similar study is performed by varying the feed-down contribution by changing the cuts on the impact parameter b_{x} and b_{y} (Δx and Δy) of the proton tracks (Fig. 7,c) and Λ candidates (Fig. 7,d). One finds that R_{G} changes maximally between $3.02 - 3.13$ fm ($2.92 - 3.23$ fm), if the contributions to the protons (Λ) from feed-down is varied between $17 - 25$ % ($39 - 46$ %).

The dependence of the radius parameter on the region in q_{inv} that is used to determine the normalization constant N (see Eq. (2)) is investigated by varying the size and position of this region. It is found that R_{G} changes by maximally ± 0.11 fm.

By taking the quadratic sum of the different contributions a total systematic error on R_{G} of $+0.44$ fm and -0.16 fm is estimated.

Another source of systematic uncertainty of the extracted radius parameter arises from the limited precision of the knowledge of the scattering lengths and effective ranges used in the calculation of the theoretical correlation function. Therefore, the fits were repeated with d_0^{S}, d_0^{T}, f_0^{S}, and f_0^{T} taken from [17, 18, 20, 22, 23, 25, 35]. The largest deviation from the R_{G} value obtained with the standard parameter set [10] is observed when using the parameters extracted by the COSY-11 collaboration [17]. While in all other cases the difference is smaller than ± 0.1 fm, it is found to be $+0.274$ fm for the COSY-11 parameters which is still close to our statistical error. Therefore we conclude that the choice of the parameters describing the p $-$ Λ interaction has a negligible effect on the final result.
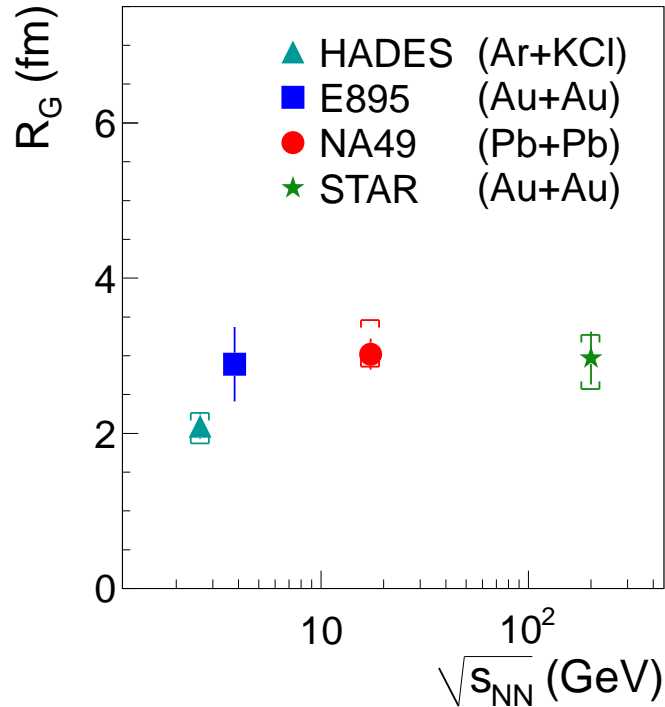
FIG. 8: The effective radius parameter R_G for p $-$ Λ correlations as a function of center of mass energy $\sqrt{s_{NN}}$. The figure also includes data on Ar+KCl collisions by the HADES collaboration [28] and on central Au+Au collisions by the E895 [7] and the STAR [29] experiments. The systematic errors are represented by the brackets. Please note that the STAR result corresponds to a slightly higher pair $\langle m_t \rangle$ than for the NA49 measurement. Assuming the m_t dependence shown Fig. 9 the STAR data point would move up by ≈ 6 %, if it was measured at the same $\langle m_t \rangle$.

C. Energy dependence of the effective radius parameter

The result of this study is compared to data at lower and higher center-of-mass energies in Fig. 8. Good agreement with the effective radius parameters measured for central Au+Au collisions by the E895 collaboration at $\sqrt{s_{NN}} = 3.83$ GeV [7] and by the STAR experiment at $\sqrt{s_{NN}} = 200$ GeV [29] is observed, indicating that there is no significant change from AGS to RHIC energies. A similar observation was made for correlations of identical charged pions [3].

At even lower energies ($\sqrt{s_{NN}} = 2.61$ GeV) the HADES collaboration measured a significantly smaller effective radius parameter for p$-$$\Lambda$ correlations of $R_G = 2.09 \pm 0.16$(stat.) fm [28]. However, the fireball volume in the case of Ar+KCl collisions is expected to be smaller

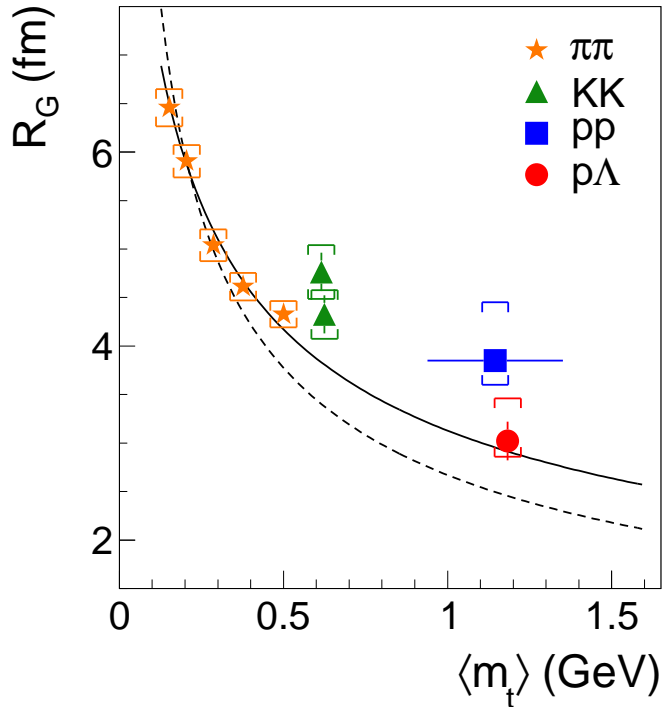FIG. 9: The effective radius parameter R_G extracted from the correlation functions of $\pi^-\pi^-$ [3], K^+K^+ and K^-K^- [8], pp [4], and p $-$ Λ pairs versus $\langle m_t \rangle$ as measured by NA49 for central Pb+Pb collisions at $\sqrt{s_{NN}} = 17.3$ GeV. The systematic errors are represented by the brackets. For explanation of curves see text.

than for Pb+Pb and Au+Au collisions. In fact, it was demonstrated in [28] that the measured p$-\Lambda$ radius parameter is dominated by the reaction geometry and scales approximately as $A^{1/3}$, irrespective of center-of-mass energy. A comparable observation was previously made for two-proton correlations in the target fragmentation region [6].

D. $\langle m_t \rangle$ dependence of the effective radius parameter

Figure 9 shows a comparison of R_G, as determined in this analysis from the p $-$ Λ correlation function, to radius parameters derived from correlations of π^- pairs [3] and charged kaon pairs [8], as well as from two-proton correlations [4], at different average transverse masses $\langle m_t \rangle$. In case of the $\pi^-\pi^-$ and KK correlations, R_G was calculated from

16

the three-dimensional radius parameter components as:

$$R_{\text{G}} = (R_{\text{side}} R_{\text{out}} R_{\text{long}})^{1/3}. \tag{6}$$

The decrease of the effective radius parameters with increasing transverse mass is generally attributed to the presence of collective flow in the fireball. The measurement of the $\text{p} - \Lambda$ correlation allows to extend this study to higher $\langle m_{\text{t}} \rangle$. In fact, R_{G} for $\text{p} - \Lambda$ pairs is significantly smaller than the effective radius parameter extracted for pions and kaons at lower $\langle m_{\text{t}} \rangle$ and is thus in agreement with the expected behavior. The dashed curve in Fig. 9 corresponds to a simple $\propto \langle m_{\text{t}} \rangle^{-1/2}$ dependence. The solid line is based on the following m_{t} dependences of the three radius components, as suggested by hydrodynamical approaches [39–41]:

$$R_{\text{side}}^2 = R_{\text{geo}}^2 / (1 + (m_{\text{t}}/T) \, \eta_{\text{f}}^2) \tag{7}$$

$$R_{\text{out}}^2 = R_{\text{side}}^2 + \beta_{\text{t}}^2 \, \Delta\tau^2 \tag{8}$$

$$R_{\text{long}}^2 = \tau_0^2 \, (T/m_{\text{t}}). \tag{9}$$

Here R_{geo} is the transverse size of the particle source, $\beta_{\text{t}} = v_{\text{f}}/c$ the transverse flow velocity, η_{f} the transverse flow rapidity $\eta_{\text{f}} = (1/2) \, \log(1 + v_{\text{f}})/(1 - v_{\text{f}})$, T the kinetic freeze-out temperature, τ_0 the total lifetime of the source and $\Delta\tau$ the emission duration. Under the assumption that all particle species freeze out from the same expanding source, we calculate R_{G} from Eq. (6), using Eqs. (7)–(9). The solid curve in Fig. 9 corresponds to the parameter $\eta_{\text{f}} = 0.8$, $\tau_0 = 0.6$ fm/c, $\Delta\tau = 3.4$ fm/c and $T = 90$ MeV, as extracted by fits with a blast wave model to the pion correlations [3]. The overall normalization has been adjusted to fit the data. A reasonable description of the effective radius parameters for most particle species can thus be achieved, with the notable exception of the two-proton correlation.

IV. SUMMARY

We report on the measurement of the $\text{p} - \Lambda$ correlation function in momentum space for central Pb+Pb collisions at $\sqrt{s_{\text{NN}}} = 17.3$ GeV. The $\text{p} - \Lambda$ pairs exhibit a clear positive correlation for small relative momenta. By comparison to a calculated correlation function a one-dimensional Gaussian source size parameter of $R_{\text{G}} = 3.02 \pm 0.20(\text{stat.})^{+0.44}_{-0.16}(\text{syst.})$ fm is determined. This value is in good agreement with measurements for Au+Au collisions at

lower and higher center-of-mass energies. The $\langle m_t \rangle$ dependence of the effective $p - \Lambda$ radius parameter follows the expectation for an expanding source as described by hydrodynamics, when compared to other two-particle correlation results.

Acknowledgments

[1] S. Pratt, Phys. Rev. D **33**, 1314 (1986).

[2] G.F. Bertsch, Nucl. Phys. A **498**, 173c (1989).

[3] C. Alt at al. (NA49 Collaboration), Phys. Rev. C **77**, 064908 (2008).

[4] H. Appelshäuser et al. (NA49 Collaboration), Phys. Lett. B **467**, 21 (1999).

[5] H. Bøggild et al. (NA44 Collaboration), Phys. Lett. B **458**, 181 (1999).

[6] T.C. Awes et al. (WA80 Collaboration), Z. Phys. C **65**, 207 (1995).

[7] P. Chung et al. (E895 Collaboration), Phys. Rev. Lett. **91**, 162301 (2003).

[8] S.V. Afanasiev et al. (NA49 Collaboration), Phys. Lett. B **557**, 157 (2003).

[9] B.I. Abelev et al. (STAR Collaboration), Phys. Rev. C **74**, 054902 (2006).

[10] F. Wang and S. Pratt, Phys. Rev. Lett. **83**, 3138 (1999).

[11] G. Alexander et al., Phys. Rev. **173**, 1452 (1968).

[12] B. Sechi-Zorn et al., Phys. Rev. **175**, 1735 (1968).

[13] J.A. Kadyk et al., Nucl. Phys. B **27**, 13 (1971).

[14] O.I. Dahl et al., Phys. Rev. Lett. **6**, 142 (1961).

[15] D. Cline et al., Phys. Rev. Lett. **20**, 1452 (1968).

[16] O. Braun et al., Nucl. Phys. B **124**, 45 (1977).

[17] J.T. Balewski et al. (COSY-11 Collaboration), Eur. Phys. J. A **2**, 99 (1998).

[18] A. Budzanowski et al. (HIRES Collaboration), Phys. Lett. B **687**, 31 (2010).

[19] M.M. Nagels, Th.A. Rijken, and J.J. de Swart, Phys. Rev. D **20**, 1633 (1979).

[20] A.R. Bodmer and Q.N. Usmani, Nucl. Phys. A **477**, 621 (1988).

[21] P.M.M. Maessen, Th.A. Rijken, and J.J. de Swart, Phys. Rev. C **40**, 2226 (1989).

[22] Th.A. Rijken, V.G.J. Stoks, and Y. Yamamoto, Phys. Rev. C **59**, 21 (1999).

[23] J. Haidenbauer and U.G. Meißner, Phys. Rev. C **72**, 044005 (2005).

[24] H. Polinder, J. Haidenbauer, and U.G. Meißner, Nucl. Phys. A **779**, 244 (2006).

[25] A. Sibirtsev et al., Eur. Phys. J. A **27**, 269 (2006).

[26] C. Blume et al. (for the NA49 Collaboration), Nucl. Phys. A **715**, 55c (2003).

[27] H. Beck, Dipl. thesis, Univ. Frankfurt (2009), https://edms.cern.ch/file/1110981/1/Hans_Beck.pdf.

[28] G. Agakishiev et al. (HADES Collaboration), Phys. Rev. C **82**, 021901(R) (2010).

[29] J. Adams et al. (STAR Collaboration), Phys. Rev. C **74**, 064906 (2006).

[30] S. Afanasiev et al. (NA49 Collaboration), Nucl. Instrum. Meth. A **430**, 210 (1999).

[31] C. Alt et al. (NA49 Collaboration), Phys. Rev. C **78**, 034918 (2008).

[32] T. Anticic et al. (NA49 Collaboration), Phys. Rev. C **80**, 034906 (2009).

[33] C. Amsler et al. (Particle Data Group), Phys. Lett. B **667**, 1 (2008).

[34] T. Anticic et al. (NA49 Collaboration), Phys. Rev. C **83**, 014901 (2011).

[35] R. Lednickỳ, *arXiv*:nucl-th/0112011.

[36] F. Becattini, J. Manninen, and M. Gaździcki, Phys. Rev. C **73**, 044905 (2006).

[37] Geant—Detector Description and Simulation Tool, CERN Program Library Long Writeup W5013.

[38] R. Lednickỳ and V.L. Lyuboshits, Sov. J. Nucl. Phys. **35**, 770 (1982).

[39] U. Wiedemann and U. Heinz, Phys. Rep. **319**, 145 (1999).

[40] S. Chapman, P. Scotto and U. Heinz, Heavy Ion Phys. **1**, 1 (1995).

[41] A.N. Makhlin and Y.M. Sinyukov, Z. Phys. C **39**, 69 (1988).